

# Comparison of short-range-order in liquid- and rotator-phase states of a simple molecular liquid: A reverse Monte Carlo and molecular dynamics analysis of neutron diffraction data

Luis Carlos Pardo, Josep Lluís Tamarit, and Nestor Veglio

*Departament de Física i Enginyeria Nuclear, Laboratori de Caracterització de Materials, Escola Tècnica Superior d'Enginyeria Industrial de Barcelona Universitat Politècnica de Catalunya, Diagonal, 647 08028 Barcelona, Catalonia, Spain*

Francisco Javier Bermejo

*Instituto de Estructura de la Materia, CSIC and Departamento Electricidad y Electrónica-Unidad Asociada CSIC, Facultad de Ciencia y Tecnología, Universidad del País Vasco/EHU, P.O. Box 644, E-48080 Bilbao, Spain*

Gabriel Julio Cuello

*Institut Laue Langevin, 6 Rue Jules Horowitz, Boîte Postale 156x, F-38042 Grenoble Cedex 9, France*

(Received 25 June 2007; revised manuscript received 7 August 2007; published 11 October 2007)

The short-range order (SRO) correlations in liquid- and rotator-phase states of carbon tetrachloride are revisited here. The correlation of some angular magnitudes is used to evaluate the positional and orientational correlations in the liquid as well as in the rotator phase. The results show significant similarities in the relative position of the molecules surrounding a central one but striking differences in their relative orientations, which could explain the changes in SRO between the two phases and the puzzling behavior of the local density in the liquid and rotator phases.

DOI: [10.1103/PhysRevB.76.134203](https://doi.org/10.1103/PhysRevB.76.134203)

PACS number(s): 61.25.Em, 61.20.-p, 61.43.-j, 61.12.-q

## I. INTRODUCTION

The detailed intermolecular structure of liquids composed by symmetric top molecules, such as carbon tetrachloride ( $\text{CCl}_4$ ), has been the subject of continued controversy since its very first determination by means of x-ray diffraction<sup>1</sup> more than half a century ago. The subject has received considerable attention over very many decades which have witnessed how the level of detail pertaining to the microscopic short-range order (SRO) of this molecular liquid has significantly increased, mainly due to the concurrence of computational techniques such as molecular dynamics (MD),<sup>2,3</sup> theoretical treatments based on the reference interaction site model (RISM),<sup>4,5</sup> as well as analysis of experimental diffraction patterns carried out by means of the reverse Monte Carlo (RMC) method.<sup>6-10</sup> The latter technique basically provides molecular configurations compatible with the measured structure factors  $S(Q)$  or its representation in the real space, the total neutron weighted radial distribution function  $G(r)$ , by means of minimization of a cost function such as the chi-squared statistic between the observed data and that calculated for a given particle configuration, subject to a number of constraints imposed by the molecular structure as well as excluded volume considerations.

The topic we address here concerns the relationship of the intermolecular structure of carbon tetrachloride within its stable liquid state and that corresponding to the fcc rotator-phase crystal which can be reached by cooling the liquid at temperatures not too low below its melting point at ambient pressure ( $T_{fcc \rightarrow L} = 245.8$  K). Such a phase is thermodynamically metastable and can be considered in terms of its free energy as having a stability close to the liquid in the sense of the Ostwald rule of states. As a matter of fact, several liquids composed by quasispherical molecules such as  $\text{CCl}_4$  as well

as all those of the methylchlorobromomethane family<sup>11</sup> display such mesophases between the liquid and the completely ordered crystalline phase, where molecules rotate fairly freely about their equilibrium lattice positions. Because of their mechanical properties, such phases have also been referred to as plastic crystals and, alternatively, are also known as orientational disordered crystals (ODICs). Within such phases, positional long-range order persists as resulting from the underlying, usually cubic, lattice defined by the time-averaged positions of the molecular centers of mass, while orientational correlations are short ranged.

Previous studies on the orientational correlations in the liquid displaying a high level of detail have been carried out by means of MD simulations,<sup>2,3</sup> RISM,<sup>4</sup> and recently also by means of RMC analysis of experimental data (see Pardo *et al.* in Ref. 10). For the fcc ODIC phases of solids composed by tetrahedral molecules  $\text{CX}_4$  [ $\text{CCl}_4$ ,<sup>2</sup> neopentane,<sup>12</sup> and  $\text{CBr}_4$  (Ref. 13)], the available evidence tells that the  $\text{CX}$  vectors are oriented along  $[110]$  and  $[100]$  cubic lattice directions, executing the molecule large-amplitude orientational excursions, the number of which is dictated by crystal and molecular point-group symmetry restrictions. Our aim here is therefore to explore the extent upon which the SRO of the plastic phases is related to that of the liquid, and thus to shed some light into the issue of the relationship between orientational and positional ordering.

## II. EXPERIMENTS AND DATA ANALYSIS

A series of neutron diffraction experiments were carried out using the D1b diffractometer at the Institut Laue Langevin, Grenoble, France. The instrument is a general purpose powder diffractometer which employs as a detector element a wide banana-shaped array covering a wide angular range.

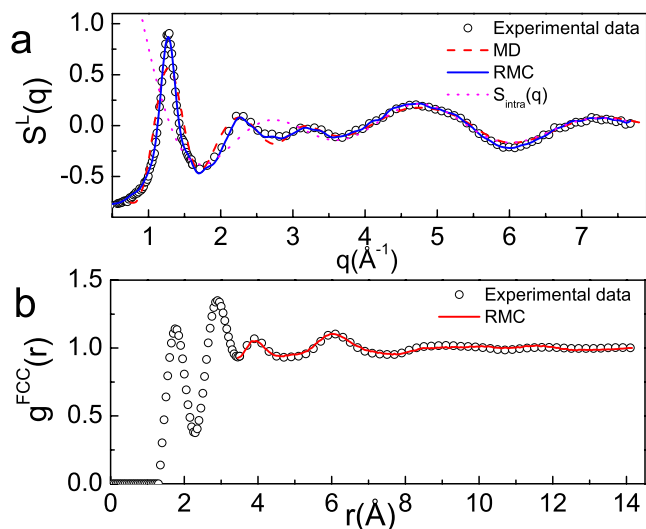


FIG. 1. (Color online) (a) Experimental structure factor (circles) for the liquid phase compared with that obtained using RMC (solid line) and molecular dynamics (dashed line). The dotted line is the molecular structure factor. (b) Experimental total radial distribution function (circles) compared with that obtained via RMC fitting (solid line).

The measurements employed a wavelength  $\lambda=1.2805$   $\text{\AA}$  which, when combined with the data acquisition at two different detector positions, allowed us to cover a reciprocal space range, large enough to study the intermolecular structure factor. Details concerning the instrument settings and data correction procedures are given elsewhere.<sup>10</sup> The ODIC phase was prepared *in situ* following procedures already described.<sup>10</sup> The growth of a polycrystalline fcc phase was ascertained by the emergence of a set of crystalline Bragg peaks as described previously (see Ref. 10).

In order to extract the maximum information from the neutron diffraction patterns, we have performed a RMC analysis of the obtained data on both phases, liquid and ODIC, using the RMCA code developed by McGreevy.<sup>6</sup> In both cases, as well as in the case of the molecular dynamics simulations, flexible molecules have been used, being their initial geometry determined by *ab initio* calculations.<sup>3</sup> The total structure factor for the liquid at  $T=298$  K was analyzed by RMC analysis using a simulation box composed by 1000 molecules, with dimensions set to reproduce the experimental density of the liquid ( $L=54.34$   $\text{\AA}$ ). As it has been shown before, the agreement between the spectra simulated from the RMC configurations and the experimental  $S(Q)$  is excellent [see Fig. 1(a)]. Such an agreement also extends to the  $S(Q)$  calculated from configurations obtained from a previous MD simulation<sup>3</sup> [see Fig. 1(a)]. We have also plotted in Fig. 1(a) the intramolecular contribution to the total structure factor calculated from the *ab initio* simulation.<sup>3</sup> As it is clearly seen in the figure, for  $q > 4$   $\text{\AA}^{-1}$ , the only significant contribution is that related to the molecular geometry, being that a confirmation that the scan in the reciprocal space is enough to determine the intermolecular structure factor. However, in order to check the reliability of our data, we have made a fitting of the intramolecular contribution to the

structure factor for  $q > 4$   $\text{\AA}$ , obtaining a distance between the carbon atom and the chlorine of 1.763  $\text{\AA}$  (Cl-Cl distance is obtained from the tetrahedral molecular symmetry,  $d_{\text{Cl-Cl}} = \sqrt{8/3}d_{\text{C-Cl}}$ ), which is in full agreement with previous determinations.<sup>3</sup>

In order to obtain quantitative estimates of the orientational order within the ODIC phase at  $T=240$  K, a RMC simulation using the aforementioned software<sup>6</sup> was performed using a box containing  $6 \times 6 \times 6$  cells, with a length determined by the Bragg peaks appearing in the spectra ( $L=50$   $\text{\AA}$ ). In this case, we have followed the method proposed in Ref. 14, fitting the total radial distribution function. The RMC fitting has been performed with flexible molecules, allowing only small-amplitude motions of the molecular centers about the lattice points defined by the experiment and changing the orientations of the molecules. The agreement between fit and experiment can be seen in Fig. 1(b) (for further details, see Ref. 10). As will be shown below, the obtained results are also in full agreement with previous MD simulations. The intercomparison of RMC and MD results provides us with reassurance about the robustness of the procedures here employed for the liquid and the plastic phases, since the former is shown to account for most of the subtleties brought in by the details of the intermolecular interactions which are obviously present in the MD data.

### III. ANALYSIS OF FINAL CONFIGURATIONS

The liquid structure of  $\text{CCl}_4$  has been analyzed up to now using different tools to quantify the molecular correlations. One way to analyze the configurations obtained using whatever method (RISM, RMC, MD, etc.) relies upon the analysis of partial radial distribution functions (see Refs. 3 and 7), assuming different kinds of molecular correlations. This implies an *a priori* definition of configurations, and therefore cannot account for configurations different from those. An alternative analysis, also using the obtained partial radial distribution functions, has been proposed by Yokogawa *et al.*<sup>15</sup> in which the three-dimensional (3D) spatial distribution function is reconstructed for every atom of a molecule, surrounding a central one. Although this method can be powerfully exploited if experimental partial distribution functions are accessible, in our case the molecular configurations can be directly studied, without the loss of 3D information implied in the calculation of radial distribution functions necessary to use the method of Yokogawa's *et al.* Alternatively, one can account for the angular correlation between CX vectors of two molecules, determine the angles between three different molecular centers, or make a projection of the position of the molecular centers onto two perpendicular planes of the molecule. However, as it has already been pointed out by Jedlovsky *et al.*,<sup>16</sup> these methods except the last result in a loss of significant information since that pertaining to the 3D SRO is compressed down to one dimension. As regards the last method, it also has some drawback due to loss of information when projecting the sphere into a plane. That is, any information concerning the structure near the equatorial plane is smoothed away.

We propose in this work to extend the bivariate analysis followed in Ref. 16 to the study of the SRO in disordered

TABLE I. Position of the molecules with respect to a central molecule (angles defined in text) when placed in the symmetry axis of the molecule. For molecules placed in the poles, the  $\phi$  angle is undetermined (\*).

Positional configuration	Picture	$\cos \theta$	$\phi$
Corner type ( $C_{3v}$ )	Figs. 2(a), 3(a), and 3(b)	1, -0.33	Undetermined *, (0,120°,240°)
Face type ( $C_{3v}$ )	Figs. 2(b) and 3(c)	1, -0.33	Undetermined *, (60,180°,300°)
Edge type ( $C_{2v}$ )	Figs. 2(c) and 3(d)	0.58, -0.58	(0,120°,240°),(60,180°,300°)

phases. The method just referred not only allows us to represent in a proper way the local structure of a disordered system but also allows us to study the orientational order as a function of successive coordination shells. To perform such an analysis, we start with a molecular fixed frame of reference where the  $z$  axis is set along one C-Cl direction and the  $x$  axis along the projection of another C-Cl vector in the  $XY$  plane, i.e., a plane perpendicular to the first C-Cl vector. To quantify the relative position of two molecules, we define a vector C-C connecting the molecular centers of two molecules, being  $\theta$  the angle between the  $z$  axis and the C-C vector and  $\phi$  that between the  $x$  axis and the projection of the C-C vector onto the  $XY$  plane. In doing so, plots representing the bivariate distributions of these two angles versus the distance between molecular centers provide us with a genuine three-dimensional radial distribution function  $g_{CC}(r, \theta, \phi)$  of the molecular centers, which determines the relative position between two molecules. In addition and to specify the relative orientation of two molecules, we have also carried out a statistical analysis of the angle  $\alpha$  defined as that given by two randomly chosen C-Cl vectors of different molecules, as a function of the position of a central molecule. However, as pointed out by Blum and Torruella,<sup>17</sup> a full description of the short-range order between molecules without cylindrical symmetry needs six angular variables, three Euler angles describing the position of a molecular center with respect to a central molecule and three Euler angles describing the relative orientation of the second molecule. Here, because of the  $T_d$  point-group symmetry of the  $CCl_4$  molecule, we may fix the molecule in the aforementioned three-axis frame, and therefore only two angles are necessary to describe the position of the next molecular center ( $\theta$  and  $\phi$ ). In other words, the degree of freedom related to the rotation along the  $z$  axis is fixed placing a C-Cl vector of the molecule in the  $XZ$  plane. Therefore, this method allows a complete description of the 3D positional ordering of the molecules in the case of  $CCl_4$ .

Concerning the relative orientation of the molecule, we will only distinguish two relative orientations of two molecules by means of a unique angular parameter  $\alpha$ . We define a ferromagnetic configuration when the C-Cl vectors of two molecules are parallel ( $\cos \alpha=1$ ) and antiferromagnetic when a pair of C-Cl vectors are antiparallel ( $\cos \alpha=-1$ ). However, depending on the particularities of these configurations, i.e., tilt angle and rotation of the two molecules along the vector connecting their two centers, a second peak at least will appear in the  $\cos \alpha$  axis (see Fig. 3). Therefore, although the proposed representation of the orientational configuration of two molecules is still incomplete (we would

need another two angular variables to fully determine it), it is enough for practical purposes to describe the main difference between the orientational molecular ordering between the liquid and the plastic phase.

In order to clarify the aforementioned technique to characterize the SRO, we have summarized in Table I some possible positional ordering of  $CCl_4$  molecules, having taken into account their  $T_d$  molecular symmetry. If we consider, for example, the Corner-type configuration, for which a neighbor molecule is placed such that the C-Cl vector coincides with that joining the molecular centers [see Fig. 2(a)], the calculated value for  $\cos \theta$  should be 1 ( $\cos \theta=1$ ) and  $\phi$  is undetermined. Molecular symmetry, however, imposes that  $(\cos \theta, \phi)$  pairs  $(-0.33, 0^\circ)$ ,  $(-0.33, 120^\circ)$ , and  $(-0.33, 240^\circ)$  are also possible, being the last equivalent to  $(-0.33, 120^\circ)$  due to  $XZ$  symmetry. The  $(\cos \theta, \phi)$  pairs for the rest of the configurations are calculated in a similar way. In the first column of Fig. 3, we have plotted  $g(\cos \theta, \phi)$  assuming the positional configurations depicted in Fig. 2. In addition, in the second column,  $p(\cos \theta, \cos \alpha)$  is also shown assuming ferromagnetic or antiferromagnetic orientational ordering in order to reproduce some of the configurations found in the bibliography.

#### IV. COMPARISON BETWEEN THE SHORT RANGE ORDER IN LIQUID AND PLASTIC PHASES

In Fig. 4, we show the partial radial distribution function for the molecular centers  $g_{CC}(r)$  for the two disordered phases, liquid and ODIC, obtained for the MD simulation and the RMC fitting. As it can be seen in the figure, RMC method gives a broader distribution of molecular centers than MD (the same happens, for example, in a previous study of the water SRO<sup>18</sup>). This agrees with the well known

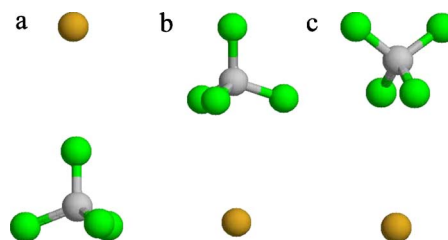


FIG. 2. (Color online) Relative position of a molecular center with respect to a central  $CCl_4$  molecule, having taken into account the symmetry axis of the molecule: along  $C_{3v}$  (a) in the corner or (b) in the face or (c) along the  $C_{2v}$  axis (see also Table I).

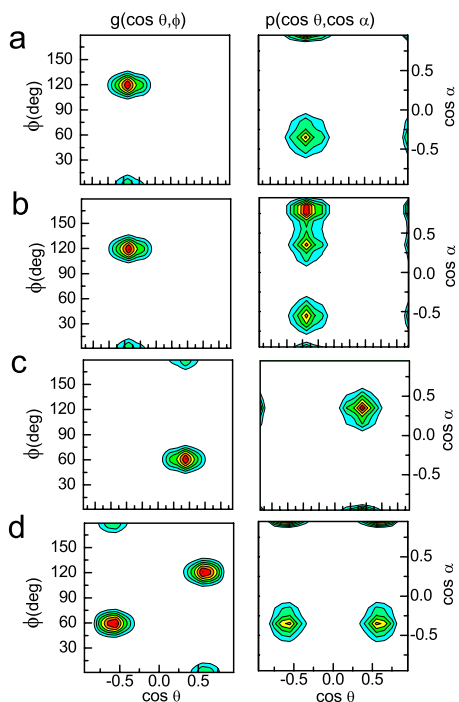


FIG. 3. (Color online) Bivariate analysis performed for some example configurations: (a) corner type with ferromagnetic orientation (Apollo configuration in Ref. 2), (b) corner type with antiferromagnetic orientation (corner to corner in Ref. 9), (c) face type with antiferromagnetic orientation (face to face in Refs. 5, 7, and 10), and (d) edge type with ferromagnetic orientation (pure interlocked in Ref. 3). Molecules placed in the  $z$  axis are not shown because of the impossibility to determine the  $\phi$  angle (see text).

fact that RMC gives the most disordered configuration compatible with the experimental results. A glance to the figure reveals that the first neighbors in the liquid phase are closer than in the fcc phase, irrespective of the method used to obtain the final configurations (RMC or MD). This implies, first, that at the very short distances, the molecular coordination number (MCN) of the liquid is higher than that of the ODIC phase, and so does the local density (see inset of Fig. 4), and second, because of the more compact arrangement of first neighbors in the liquid, the maximum of  $g_{CC}(r)$  is located at a lower distance for the liquid than for the fcc phase. To investigate up to what extent this is related to peculiarities in the SRO, we show in Fig. 5 the  $g_{CC}(\cos \theta, \phi)$  function using the aforementioned bivariate representation which was constructed in the following way. Accounting for the calculated MCN (Fig. 4) for the liquid, we define concentric shells comprised between two distances  $r_i$  and  $r_f$  as those containing the first, second, third, and so on molecules. This somewhat arbitrary definition does not affect the following discussion, since we are interested on possible changes of SRO as a function of distance. Using this definition, we then calculate the probability function  $g_{CC}(\cos \theta, \phi)$  for successive shells. Because of the positional ordering of the fcc crystal, the first shell corresponds to the 12 nearest neighbors. For the sake of clarity and to improve statistics, in Fig. 5, we have grouped together shells showing similar patterns for the liquid. To highlight some further details concerning Fig. 5,

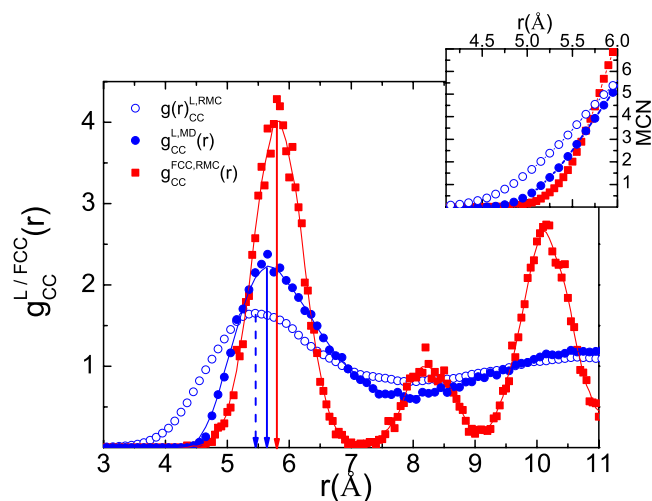


FIG. 4. (Color online)  $g_{CC}(r)$  obtained via MD and RMC fitting of the experimental data for both the liquid phase (filled and empty circles) and the fcc phase (full squares). In the inset, the molecular coordination number (MCN) is shown for the distances where local density of the liquid is higher than that of the plastic phase.

see Table I which gives relative positions along all the symmetry axes of the  $CCl_4$  molecule as  $(\cos \theta, \phi)$  pairs. If we now have a look at Fig. 5, we see that the first four neighbors are placed opposite to the faces of a central molecule [Fig. 5(a)], the next four neighbors are placed either in the corner or in the edges of the central molecule [Fig. 5(b)], and the last four neighbors are placed in the corners of the central molecule [Fig. 5(c)]. This means that within the first peak of the  $g_{CC}(r)$  function, a dramatic change in SRO happens, and therefore, analysis of SRO taking into account all the first 12 neighbors would lead only to partial conclusions (a similar conclusion has very recently been obtained by Rey<sup>19</sup>). If we now plot  $g_{CC}(\cos \theta, \phi)$  for the plastic phase, the pattern obtained is very similar to that obtained for the liquid, i.e., for

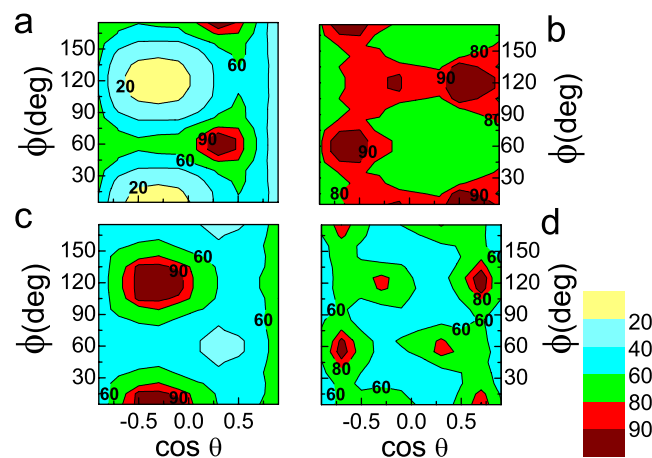


FIG. 5. (Color online) 3D distribution function of molecular centers,  $g_{CC}(\cos \theta, \phi)$ , (a) for the first four neighbors, (b) for the next four neighbors, and (c) for the last four neighbors within the first peak of  $g_{CC}(r)$ . (d)  $g_{CC}(\cos \theta, \phi)$  is also shown for the fcc phase.

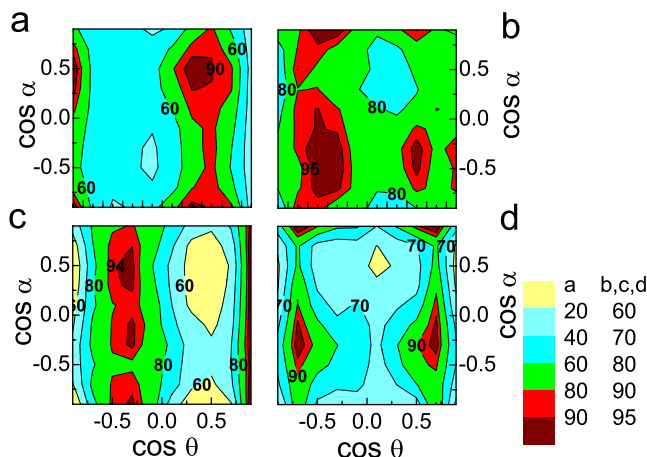


FIG. 6. (Color online) Bivariate analysis  $P(\cos \alpha, \cos \theta)$  for neighbors (a) 1–4, (b) 5–8, and (c) 9–12 in the liquid phase and also for (d) the fcc phase.

the ODIC, the relative position of a molecule given a central one mimics that of the liquid phase. Here, it is worth pointing out that our results are in complete agreement with the aforementioned previous MD simulations (C-X vectors lie along  $[110]$  and  $[100]$  directions), although in Fig. 5(d), we show a different representation of the SRO for a molecule in a lattice.<sup>2,12,20</sup> To make this point clear, we can see in Fig. 5 spots at  $(-0.33, 0^\circ)$  and  $(0.33, 60^\circ)$ , which means that molecules are placed in the corners and faces (see Table I) with respect of the first neighbors, which are just that in the  $[110]$  directions. Molecules oriented along the  $[100]$  directions are represented at the spots  $(0.7, 0^\circ)$  and  $(-0.7, 60^\circ)$  and would correspond to the molecules placed in the edge of the molecules in the liquid phase represented by the large spots at about  $(0.58, 0^\circ)$  and  $(-0.58, 60^\circ)$ .

Up to now, we have only calculated, given a central molecule, the most probable position for which a second  $\text{CCl}_4$  molecule can be found, but we still have no information concerning the relative orientation of the two molecules. That has been usually obtained by means of statistical analyses of the aforementioned  $\alpha$  angle between two randomly chosen C-Cl vectors of different molecules, but collapsing this information for all relative molecular positions, i.e., using  $P(\cos \alpha)$ .<sup>7,10</sup> Here, using the bivariate analysis, we can discriminate the relative orientation of two molecules ( $\cos \alpha$ ) as a function of its position ( $\cos \theta$ ), i.e.,  $P(\cos \theta, \cos \alpha)$ . As we have previously argued, we will distinguish between two possible main orientations only: ferromagnetic ( $\cos \alpha = 1$ ) and antiferromagnetic ( $\cos \alpha = -1$ ). With this additional information in mind, we will also be able to compare with previous determinations of the SRO. In Fig. 6, we can see that the relative orientation of the first four neighbors is antiferromagnetic, and as shown in Fig. 5, these are placed on the face of the molecule, which is the face-to-face-type configuration found in previous works.<sup>5,7,10</sup> For the next four neighbors, the orientation is ferromagnetic, and these are

placed at the edges and corners of the molecule, giving rise to the previously determined pure interlocked<sup>3</sup> and Apollo<sup>2</sup> (i.e., two molecules with the C-Cl vectors parallel) configurations. The last four neighbors [Fig. 6(c)] are antiferromagnetically oriented, giving rise to the corner to corner configuration assigned to the SRO by J3v3ari *et al.*<sup>9</sup> Therefore, we can conclude that to obtain a correct picture of the SRO, it is very important to perform some kind of “distance sensitive” analysis; otherwise, as it happened with the aforementioned previous determinations, depending on the sensibility of the analysis to a determined feature, a different kind of SRO will be obtained.

Figure 6(d) shows also the angular correlation for the nearest neighbors within the ODIC phase. Although a similar positional SRO (see Fig. 5) has been found for the liquid phase, we can see in this figure that the relative orientation of molecules is opposite to that for the first coordination shell in the liquid, that is, only the spots corresponding to ferromagnetic alignment are present in the fcc phase. That would explain the aforementioned “local density paradox:” although an antiferromagnetic alignment of the molecules allows a maximal proximity and a minimal dimer configuration energy,<sup>10</sup> this relative orientation of the molecules does not allow the formation of a fcc lattice, in which we have proved that molecules jump between sites keeping dynamically their relative ferromagnetic orientation. Therefore, the transition between the liquid and the ODIC phase would imply mainly only a change in the relative orientation of the four nearest neighbors and the last four neighbors within the first  $g_{\text{CC}}^{\text{liquid}}(r)$  peak, from an antiferromagnetic alignment to a ferromagnetic alignment, which would allow stacking of the molecules, and therefore the long-range order formation in the plastic phase.

## V. CONCLUSIONS

In conclusion, this study shows, first, how the short-range order for the liquid phase for a simple molecular liquid, such as  $\text{CCl}_4$ , is remarkably much more complex than that reported up to now. Second, it explains the local and/or macroscopic density paradox evidenced by the partial radial distribution function of molecular centers shown in Fig. 4. Although in both phases the positional SRO is approximately the same, the orientational SRO changes between the two phases: While the liquid phase simply minimizes the distance and configurational energy forming an antiferromagnetic configuration, the ferromagnetic configuration in the ODIC phase allows a dynamically disordered stacking of molecules which yields the formation of a long-range ordered lattice.

## ACKNOWLEDGMENTS

We would like to acknowledge R. Rey for the MD configurations used in this work. We would also like to acknowledge “Generalitat de Catalunya” (Project No. 2005SGR-00535) and MEC (Project No. FIS2005-00975) for partial support of this work.

- <sup>1</sup>A. Eisenstein, Phys. Rev. **63**, 304 (1943).
- <sup>2</sup>I. McDonald, D. G. Bounds, and M. L. Klein, Mol. Phys. **45**, 521 (1982).
- <sup>3</sup>R. Rey, L. C. Pardo, E. Llanta, K. Ando, D. O. López, J. Ll. Tamarit, and M. Barrio, J. Chem. Phys. **112**, 7505 (2001).
- <sup>4</sup>L. J. Lowden and D. Chandler, J. Chem. Phys. **61**, 5228 (1974).
- <sup>5</sup>S. Tomonari and H. Sekino, J. Chem. Phys. **125**, 034509 (2006); N. Minezawa and S. Kato, *ibid.* **126**, 054511 (2007).
- <sup>6</sup>For reviews on applications of the method see R. L. McGreevy, J. Phys.: Condens. Matter **13**, R877 (2001); G. Evrard and L. Pusztai, J. Phys.: Condens. Matter (Special Issue) **17**, S1 (2005).
- <sup>7</sup>P. Jedlovsky, J. Chem. Phys. **107**, 7433 (1997).
- <sup>8</sup>L. Pusztai and R. L. McGreevy, Mol. Phys. **90**, 533 (1997).
- <sup>9</sup>P. Jónvári, G. Meszáros, L. Pusztai, and E. Sváb, J. Chem. Phys. **114**, 8082 (2001).
- <sup>10</sup>N. Veglio, F. J. Bermejo, L. C. Pardo, J. L. Tamarit, and G. J. Cuello, Phys. Rev. E **72**, 031502 (2005); L. C. Pardo, N. Veglio, F. J. Bermejo, J. L. Tamarit, and G. J. Cuello, Phys. Rev. B **72**, 014206 (2005).
- <sup>11</sup>L. C. Pardo, M. Barrio, J. Ll. Tamarit, D. O. López, J. Salud, and H. A. J. Oonk, Chem. Mater. **17**, 6146 (2005); L. C. Pardo, M. Barrio, J. Ll. Tamarit, D. O. López, J. Salud, P. Negrier, and D. Mondieig, J. Phys. Chem. **105**, 10326 (2001); Phys. Chem. Chem. Phys. **3**, 2644 (2001).
- <sup>12</sup>W. Breymann and R. M. Pick, J. Chem. Phys. **91**, 3119 (1989).
- <sup>13</sup>M. T. Dove, J. Phys. C **19**, 3325 (1986).
- <sup>14</sup>L. Karlsson and R. L. McGreevy, Physica B **234-236**, 100 (1997).
- <sup>15</sup>D. Yokogawa, H. Sato, and S. Sakaki, J. Chem. Phys. **125**, 114102 (2006).
- <sup>16</sup>P. Jedlovsky, A. Vincze, and G. Horvai, Phys. Chem. Chem. Phys. **6**, 1874 (2004).
- <sup>17</sup>L. Blum and A. J. Torruella, J. Chem. Phys. **56**, 303 (1972).
- <sup>18</sup>P. Jedlovsky, J. P. Brodholt, F. Bruni, M. A. Ricci, A. K. Soper, and R. Vallauri, J. Chem. Phys. **108**, 8528 (1998).
- <sup>19</sup>R. Rey, J. Chem. Phys. **126**, 164506 (2007).
- <sup>20</sup>M. More, J. Lefebvre, B. Hennion, B. M. Powell, and C. M. E. Zeyen, J. Phys. C **13**, 2833 (1980).